Ultrasound Enhanced Enzymatic Hydrolysis of Parthenium hysterophorus: A Mechanistic Investigation

ARTICLE *in* BIORESOURCE TECHNOLOGY · JUNE 2015

Impact Factor: 4.49 · DOI: 10.1016/j.biortech.2015.06.031

5 AUTHORS, INCLUDING:

Mayank Agarwal
Indian Institute of Technology Guwahati
4 PUBLICATIONS **10** CITATIONS

Bioresource Technology 192 (2015) 636–645

Contents lists available at ScienceDirect

Bioresource Technology

journal homepage: www.elsevier.com/locate/biortech

Ultrasound enhanced enzymatic hydrolysis of *Parthenium hysterophorus*: A mechanistic investigation

Shuchi Singh [a], Mayank Agarwal [b], Aditya Bhatt [c], Arun Goyal [a,d], Vijayanand S. Moholkar [a,b,*]

[a] Center for Energy, Indian Institute of Technology Guwahati, Guwahati 781 039, Assam, India
[b] Department of Chemical Engineering, Indian Institute of Technology Guwahati, Guwahati 781 039, Assam, India
[c] Department of Chemical Engineering, National Institute of Technology Tiruchirappalli, Tiruchirappalli 620 015, Tamil Nadu, India
[d] Department of Biosciences and Bioengineering, Indian Institute of Technology Guwahati, Guwahati 781 039, Assam, India

HIGHLIGHTS

- Mechanistic investigations of ultrasonic enzymatic hydrolysis using HCH-1 model.
- Optimization of enzymatic hydrolysis of pretreated and delignified biomass.
- 6× and 20% enhancement in hydrolysis kinetics and sugar yield, respectively.
- Micro-convection enhances enzyme/substrate affinity and reaction velocity.
- Sonication reduces product inhibition of free, adsorbed and complexed enzyme.

GRAPHICAL ABSTRACT

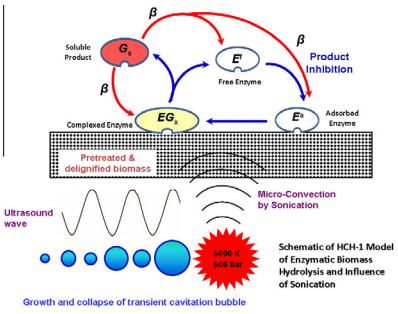

ARTICLE INFO

Article history:
Received 16 May 2015
Received in revised form 5 June 2015
Accepted 6 June 2015
Available online 12 June 2015

Keywords:
Hydrolysis
Sonication
Reducing sugar
Cavitation
P. hysterophorus

ABSTRACT

This study has attempted to establish the mechanism of the ultrasound-induced enhancement of enzymatic hydrolysis of pretreated and delignified biomass of *Parthenium hysterophorus*. A dual approach of statistical optimization of hydrolysis followed by application of sonication at optimum conditions has been adopted. The kinetics of hydrolysis shows a marked 6× increase with sonication, while net sugar yield shows marginal rise of ~20%. The statistical experimental design reveals the hydrolysis process to be enzyme limited. Profile of sugar yield in ultrasound-assisted enzymatic hydrolysis has been analyzed using HCH-1 model coupled with Genetic Algorithm optimization. The trends in the kinetic and physiological parameters of HCH-1 model reveal that sonication enhances enzyme/substrate affinity and reaction velocity of hydrolysis. The product inhibition of enzyme in all forms (free, adsorbed, complexed) also reduces with ultrasound. These effects are attributed to intense micro-convection induced by ultrasound and cavitation in the liquid medium.

1. Introduction

Fast depletion of fossil fuel reserves has posed daunting threat to global energy security. Moreover, emission of greenhouse gases from industrial and vehicular exhaust has also raised serious concerns of global warming and climate change risks. As a common solution to both issues of energy security and climate change, the production of alternate liquid biofuels, which could substitute the fossil fuels, has been an immensely active research area for last one decade. Alcoholic biofuels such as bioethanol and biobutanol produced through fermentation route can be blended with crude oil derived liquid transportation fuels of gasoline and diesel. The

* Corresponding author at: Department of Chemical Engineering, Indian Institute of Technology Guwahati, Guwahati 781 039, Assam, India. Tel.: +91 361 258 2258; fax: +91 361 258 2291.
E-mail address: vmoholkar@iitg.ernet.in (V.S. Moholkar).

http://dx.doi.org/10.1016/j.biortech.2015.06.031
0960-8524/

production cost of alcoholic biofuels is a major function of cost of substrate or feedstock for fermentation. Lignocellulosic biomass in the form of agricultural and forest residues and waste biomasses such as grasses and weeds have been explored as the potential low-cost feedstock for fermentation. The waste biomass of *Parthenium hysterophorus* has recently attracted attention of researchers, due to its widespread availability and destructive and hazardous nature. Invasion of this weed can affect the vegetation and below-ground soil nutrients of a land (Timsina et al., 2011). Consumption of *P. hysterophorus* by animals causes loss of skin pigmentation, dermatitis and degenerative changes in some visceral organs. Prolonged exposure of a person to *P. hysterophorus* plant could result in symptoms of skin inflammations and respiratory problems (Patel, 2011). Several studies have been published that report effective utilization of this waste biomass for biofuels production (Ghosh et al., 2013; Rana et al., 2013; Pandiyan et al., 2014).

The process of conversion of lignocellulosic biomass to alcoholic biofuel comprises three steps, viz. (1) acid pretreatment and delignification of raw biomass, (2) enzymatic hydrolysis of pretreated biomass, and (3) fermentation of pentose/hexose hydrolyzates obtained from step 1 and 2 for alcohol production. Intensification of pretreatment and fermentation process with novel techniques is also a potential solution to reduction of production cost of alcoholic biofuels (Beszédes et al., 2011; Palacios-Bereche et al., 2014; Suresh et al., 2014; Bharadwaja et al., 2015). Among the three steps of alcoholic biofuel production process, the enzymatic hydrolysis of pretreated biomass is not only cost intensive (due to high cost of enzymes) but also has slow kinetics. Therefore, optimization and intensification of this step is crucial to enhancing the efficiency and capacity (or throughput) of the biofuels production process.

Ultrasound has been known for intensification of several physical, chemical and biological processes. In our earlier investigations in the subject of ultrasound assisted synthesis of biofuels, we have dealt with ultrasonic enhancement of biomass (rice straw) pretreatment by acid hydrolysis (Suresh et al., 2014), ultrasonic delignification (Singh et al., 2014a) and fermentation (Singh et al., 2015a,b). Several authors have addressed the matter of ultrasound assisted enzymatic hydrolysis using either pure substrates (Sulaiman et al., 2013; Subhedar and Gogate, 2014), or lignocellulosic substrates (Lunelli et al., 2014; Subhedar et al., 2015). Sonication (or ultrasound irradiation) of the reaction mixture causes intensification of the process through several physical and chemical effects, which are attributed to phenomenon of transient cavitation. Cavitation can be defined as nucleation, growth and transient implosive collapse of tiny gas/vapor bubbles driven by sinusoidal variation in bulk pressure induced propagation of ultrasound wave. Transient collapse of cavitation bubble causes immense energy concentration on an extremely short temporal and spatial scale (Suslick, 1990). The physical effect associated with transient cavitation is generation of high intensity micro–convection in the system, while the chemical effect associated with transient cavitation is generation of radical species through dissociation of gas/vapor molecules in the bubble at the extreme conditions of temperature and pressure reached in the bubble at transient collapse. These radicals induce and accelerate various chemical reactions in the bulk liquid medium. The propagation of ultrasound wave also causes oscillatory motion of the fluid elements of the liquid medium, which induces micro–mixing in the medium. Although previous studies have reported enhancement of enzymatic hydrolysis of biomass with ultrasound, the focus of these studies is more on results than rationale. The ultrasound–induced enhancement has been broadly attributed to physical and chemical effects of cavitation, but the exact links between physics/chemistry of ultrasound/-cavitation and the biochemistry of enzymatic hydrolysis have not been established yet.

The objective of this study is mechanistic investigation in ultrasound–assisted intensification of enzymatic hydrolysis. This investigation is preceded by optimization of the process under conventional technique of mechanical agitation using statistical design of experiments. Our approach has been to couple experimental results (under both mechanical agitation and ultrasound irradiation) with the HCH-1 model for enzymatic cellulose hydrolysis. This model takes into account the adsorption of the enzyme on cellulose, complexation of the enzyme with cellulose and transformation of the complex into soluble product. Moreover, the inhibition of enzyme in all three forms (free, adsorbed and complexed) by the product has also been accounted for. The experimental results of enzymatic hydrolysis of pretreated biomass of *P. hysterophorus* have been fitted to the HCH-1 model to obtain values of different kinetic and physiological parameters in the model using Runge–Kutta ODE solver coupled with Genetic Algorithm code. The variations or trends in the kinetic and physiological parameters of the mathematical model under conditions of mechanical agitation and ultrasound irradiation (or sonication) have given an interesting mechanistic account of the mechanism of influence of ultrasound on enzymatic hydrolysis process, as described in the subsequent sections.

For interested readers in this subject area, we would like to state that we have adopted this approach for mechanistic investigations of many biochemical systems such as ultrasound enhanced glycerol bioconversion (Khanna et al., 2012, 2013), enzymatic decolorization/degradation of textile dyes (Patidar et al., 2012; Malani et al., 2013) and ethanol fermentation with protocols of SHF (Separate Hydrolysis and Fermentation, Singh et al., 2015a) and SSF (Simultaneous Saccharification and Fermentation, Singh et al., 2015b). This analysis has revealed the important mechanistic facets of beneficial effects of ultrasound on these systems.

2. Methods

The experimental protocol of this study was divided in two parts: (1) optimization of enzymatic hydrolysis using statistical design of experiments under conventional conditions of mechanical agitation, and (2) intensification of enzymatic hydrolysis with ultrasound at optimized conditions determined from part 1.

2.1. Materials

Chemicals used for reagent preparation for sugar estimation were purchased from Fisher Scientific, India. Glucose (99.5% purity) was purchased from Sigma Aldrich, USA, and used as standard in sugar estimation protocols.

2.2. Biomass collection and processing

The lignocellulosic substrate of *P. hysterophorus* biomass in this study was collected from the campus of our institute. Biomass was chopped, washed with water and dried at 60 ± 3 °C for 24 h and ground to a particle size ~1 mm. Powdered biomass was pretreated with 1% (v/v) H_2SO_4 + 30 min autoclaving (Singh et al., 2014b), and the solid residue obtained was subjected to delignification by ultrasound assisted alkaline treatment (Singh et al., 2014a).

2.3. Source of enzymes

Carboxymethylcellulase (CMCase) (specific activity = 1.0 U/mg) was produced by the isolate *Bacillus amyloliquefaciens* SS35 (Singh et al., 2013, 2015c). β–glucosidase (250 U/g) produced by

Aspergillus niger (Novozyme 188) was procured from Sigma Aldrich (USA).

2.4. Optimization of enzymatic hydrolysis by central composite design (CCD)

2.4.1. Experimental design, statistical analysis and model fitting

The acid pretreated and delignified *P. hysterophorus* biomass, comprising 96.1 ± 0.6% (w/w) cellulose, was subjected to enzymatic hydrolysis by using two enzymes, viz. CMCase produced by *B. amyloliquefaciens* SS35 and β–glucosidase from *A. niger* (Novozyme 188). The enzymatic hydrolysis was carried out in sodium citrate buffer (0.05 M, pH 5.0) supplemented with different concentrations of biomass and the two enzymes. The reactions were performed in 150 mL Erlenmeyer flask with total reaction volume of 25 mL. The flasks were incubated at 30 °C and 150 rpm in an incubator shaker (Orbitek, Scigenics Biotech).

The central composite design (CCD) of experiments essentially fits a second-order polynomial model for the response variable. A three-factor, five-level design was used, in which five coded values ($-\alpha$, −1, 0, +1, $+\alpha$) were assigned to each factor. α is the extended level with value of $(2)^{3/4} = 1.682$. A 2^3 full–factorial CCD experimental design with three components, viz. concentrations of biomass, CMCase and β–glucosidase, at five coded levels was generated by Minitab statistical software (Release 15, Trial Version). This experimental design comprised 20 individual experiments ($=2^k + 2k + n_o$), where 'k' is the number of independent variables and n_o is the number of replicate runs at center point of the variables. The combinations of coded and exact values of the variables in different experiments in the central composite experimental design are given in Table 1. Each of the 20 experiments in the CCD was conducted in triplicate to assess reproducibility.

The response variable (total reducing sugar yield, mg/g pretreated and delignified biomass) was fitted with a full quadratic model (given in Eq. (1)) in order to correlate it to the experimental parameters or independent variables.

$$Y = \beta_o + \sum_{i=1}^{k} \beta_i x_i + \sum_{i=1}^{k} \beta_{ii} x_i^2 + \sum_{i \neq j} \sum_{i} \beta_{ij} x_i x_j \quad (1)$$

Notation: Y – response variable (total reducing sugar yield), k – number of factors or components, β_o – regression constant, β_i – linear coefficient, β_{ii} – quadratic coefficient and β_{ij} – interaction coefficient, x_i, x_j – coded independent variables. The coded values of the independent variables or factors (x_i or x_j in the range of −1 to +1) were obtained from the actual experimental values of these factors using Eq. (2):

$$x_i = (X_i - X_o)/\Delta X_i \quad i = 1, 2, 3, \ldots, k \quad (2)$$

where X_i is the real value of an independent variable, X_o is the value of X_i at the center point and ΔX_i is the step change. The analysis of variance (ANOVA) of the statistical experimental design and the quadratic model was done in order to assess the significance of influence of each individual factor on the response variable, and also the significance of interactions among these factors.

2.4.2. Experimental validation of optimization

The quadratic model (Eq. (1)) fitted to central composite design of experiments essentially predicted the optimum values of the factors or independent parameters for maximum yield of total reducing sugar. This result was validated by conducting enzymatic hydrolysis at optimum values of parameters (details given in the next section).

2.5. Intensification of enzymatic hydrolysis by ultrasound

Experiments for intensification of enzymatic hydrolysis by ultrasound were carried out using the optimum values of independent parameters obtained from the central composite experimental design.

For sonication of the enzymatic hydrolysis reaction mixture, an ultrasound bath (Tran–sonic T–460, Elma, Germany, 2L) with the dimensions 25 cm × 15 cm × 10 cm, operating frequency of 35 kHz and power rating of 35 W was used. The ultrasound bath was characterized for the actual power input to the liquid medium in the bath (i.e. water) and the pressure amplitude of the acoustic waves generated in the medium using calorimetric techniques. The actual power input to the bath was 18.58 W through a transducer with diameter of 4 cm. The net acoustic intensity and the acoustic pressure amplitude corresponding to these values are 1.48 W/cm^2 and 150 kPa, respectively (Sivasankar et al., 2007; Chakma and Moholkar, 2011). Sonication of the enzymatic hydrolysis reaction mixture was carried out in a duty cycle of 10% (i.e. 1 min of sonication and 9 min of mechanical shaking in every 10 min of reaction).

Table 1
Full factorial central composite design matrix of three components in coded and actual (in parentheses) values and the response of reducing sugar yield (mg/g).

Run order	Biomass concentration (g/L) (X_1)	CMCase concentration (U/g) (X_2)	β–glucosidase concentration (U/g) (X_3)	Reducing sugar yield (mg/g)	
				*Experimental	Predicted
1	+α (80.0)	0 (400.0)	0 (35.0)	256.7 ± 11.3	248.41
2	0 (42.5)	0 (400.0)	0 (35.0)	340.3 ± 12.6	360.42
3	0 (42.5)	+α (600.0)	0 (35.0)	408.6 ± 11.2	407.74
4	−1 (20.2)	−1 (281.1)	+1 (43.9)	312.4 ± 8.90	309.98
5	0 (42.5)	0 (400.0)	0 (35.0)	340.3 ± 17.4	360.42
6	+1 (64.8)	−1 (281.1)	+1 (43.9)	310.1 ± 15.3	310.54
7	−1 (20.2)	−1 (281.1)	−1 (26.1)	289.3 ± 12.4	284.36
8	−1 (20.2)	+1 (518.9)	+1 (43.9)	430.0 ± 8.70	424.21
9	0 (42.5)	0 (400.0)	0 (35.0)	364.5 ± 13.2	360.42
10	+1 (64.8)	+1 (518.9)	−1 (26.1)	300.2 ± 10.2	302.77
11	0 (42.5)	0 (400.0)	−α (20.0)	336.2 ± 9.20	334.34
12	+1 (64.8)	+1 (518.9)	+1 (43.9)	410.3 ± 17.3	415.39
13	0 (42.5)	−α (200.0)	0 (35.0)	342.7 ± 12.4	343.35
14	−α (5.0)	0 (400.0)	0 (35.0)	200.6 ± 9.30	208.68
15	0 (42.5)	0 (400.0)	0 (35.0)	364.5 ± 8.10	360.42
16	+1 (64.8)	−1 (281.1)	−1 (26.1)	334.5 ± 13.2	340.43
17	−1 (20.2)	+1 (518.9)	−1 (26.1)	256.4 ± 12.8	256.09
18	0 (42.5)	0 (400.0)	0 (35.0)	376.4 ± 18.2	360.42
19	0 (42.5)	0 (400.0)	0 (35.0)	376.4 ± 17.2	360.42
20	0 (42.5)	0 (400.0)	+α (50.0)	448.9 ± 15.3	450.58

* Experimental values are mean ± SE (n = 3).

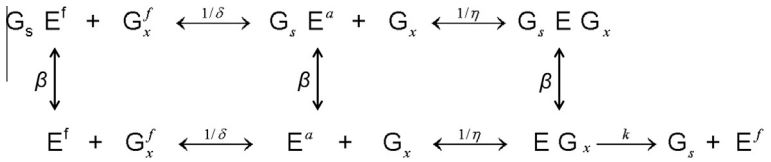

Fig. 1. Reaction mechanism for the HCH-1 model (redrawn from Holtzapple et al., 1984). (**Notation**: G_x^f – free cellulose, G_x – cellulose site G_s – soluble product, E^f – free enzyme, E^a – enzyme adsorbed on cellulose, EG_x – enzyme substrate complex, G_sE^f – inhibited free enzyme, G_sE^a – inhibited adsorbed enzyme, G_sEG_x – inhibited complexed enzyme, η – complexing constant, β – product binding constant, δ – adsorption constant, k – reaction rate constant).

The reaction flask containing enzymatic hydrolysis mixture was placed at the center of the bath. The flask was immersed to about 50% of its height in the water. The position of the flask was carefully maintained same in all experiments in view of spatial variation of the acoustic intensity in the bath (Moholkar et al., 2000, 2002). The temperature of the water in the bath was maintained at 30 ± 2 °C by replacement of small portions of initial water at regular intervals. Control experiments (mechanical shaking) were also carried out to validate the influence of ultrasound in test experiments (mechanical shaking and intermittent sonication). 200 μL aliquots of the reaction mixture were withdrawn intermittently from both control and test experiments to determine instantaneous total reducing sugar concentration. The hydrolysis treatment in both test and control experiments was carried out till the difference in the total reducing sugar content in the successive samples drawn from reaction mixture was <5%. On basis of this criterion, the hydrolysis time for control and test experiments was 96 and 14 h, respectively. Both test and control experiments were carried out in triplicate to assess the reproducibility of the results.

2.6. Lineweaver–Burk analysis of enzymatic hydrolysis process

The Lineweaver–Burk analysis of the enzymatic hydrolysis process under control and test conditions was carried out by variation of the initial biomass concentration in the hydrolysis reaction mixture. The biomass concentration was varied between 5 and 50 g/L. The concentrations of both enzymes were at their optimum values predicted by the statistical design of experiments. Other parameters such as temperature, rate of agitation and frequency/amplitude of sonication were also same as in the previous experiments. The values of enzyme kinetics parameters, viz. K_m and V_{max}, were determined using Lineweaver–Burk plots.

2.7. Analytical methods

The reducing sugar content of the samples drawn from enzymatic hydrolysis mixture was estimated by the method of Nelson (1944) and Somogyi (1945). The presence of glucose in the sample was confirmed by HPLC analysis (Perkin–Elmer, Series 200) with a refractive index detector, using HiPlex–H column (300 mm × 5 μm × 4.6 mm, Varian). Deionized water (Milli Q, HPLC grade) was used as the mobile phase at a flow rate of 0.4 mL/min. D–glucose was used as standard in these analyses.

3. Mathematical model

Holtzapple et al. (1981) and Holtzapple et al. (1984) have formulated a theoretical model for enzymatic hydrolysis of cellulose. In the experimental study that accompanied formulation of this model (Holtzapple et al., 1981), it was observed that for low substrate concentrations, some hydrolysis reactions were 1st order in substrate concentration, while others were 2nd order. 1st order substrates were finely ground and pure cellulosic materials. 2nd order substrates were coarse materials with high content of lignin and hemicellulose as impurities. This feature was independent of the size of the particles of biomass. In the context of present study, in which acid-pretreated and delignified biomass with a cellulose content of 96.1% has been used as substrate, we have used the first-order product-inhibited model by Holtzapple et al. (1984), popularly known as HCH-1 model for enzymatic cellulose hydrolysis.

The HCH-1 model hypothesizes that the first step in enzymatic hydrolysis of cellulose is adsorption of free cellulase, E^f, onto free site cellulose, G_x^f. This step is reversible and is characterized by constant, $1/\delta$. The active site of adsorbed enzyme, E^a, combines with a cellulose site to form an enzyme/substrate complex, EG_x. This step is also equilibrium limited and the equilibrium constant is given by $1/\eta$. The enzyme/substrate complex is then irreversibly transformed into the soluble product, G_s. The hydrolysis step proceeds with a rate constant, k. Assuming that decomposition of enzyme/substrate complex controls the rate of hydrolysis, the reaction velocity is written as:

$$v = k[EG_x] \tag{3}$$

The other steps are written as:

$$\frac{1}{\delta} = \frac{[E^a]}{[E^f][G_x^f]} \tag{4}$$

$$\frac{1}{\eta} = \frac{[EG_x]}{[E^a]} \tag{5}$$

It should be noted that equilibrium expression in Eq. (5) is independent of the cellulose concentration, which is an assumption of the model. This assumption is based on conjecture that for pure cellulosic materials, the surface concentration of cellulosic sites does not change with hydrolysis. The surface concentration of active sites in the hydrolyzed regions is identical with original material.

Product inhibition: Enzyme in all forms (free form, E^f, adsorbed form, E^a, and complexed form, EG_x) can complex with product to become inhibited enzyme (G_sE^f, G_sE^a or G_sEG_x). Both cellobiose and glucose can inhibit the enzyme. However, since cellobiose is a temporary intermediate product and gets transformed into glucose rather quickly, we consider herewith only the glucose inhibition, characterized by the product binding constant, β. The overall reaction mechanism is shown in Fig. 1. For simplicity, a constant for product binding is assumed for all enzyme species. A material balance on enzyme species yields:

$$\beta = \frac{[G_sE^f]}{[G_s][E^f]} \equiv \frac{[G_sE^a]}{[G_s][E^a]} \equiv \frac{[G_sEG_x]}{[G_s][EG_x]} \tag{6}$$

Inhibition factor:

$$i = \frac{1}{1 + \beta[G_s]} \tag{7}$$

A material balance on the substrate species yields following expression:

Table 2
Statistical (CCD) analysis for optimization of enzymatic hydrolysis.

Model term	Coefficient estimate	*t*–value	*p*–value
(A) Model coefficient estimated by linear, square and interaction regressions			
Intercept	360.420	69.271	0.000*
Biomass concentration (X_1)	11.813	3.422	0.007*
CMCase concentration (X_2)	19.144	5.546	0.000*
β–glucosidase concentration (X_3)	34.559	10.011	0.000*
Biomass × Biomass (X_1^2)	−46.625	−13.874	0.000*
CMCase × CMCase (X_2^2)	5.348	1.591	0.143
β–glucosidase × β–glucosidase (X_3^2)	11.328	3.371	0.007*
Biomass × CMCase ($X_1 \times X_2$)	−2.347	−0.520	0.614
Biomass × β–glucosidase ($X_1 \times X_3$)	−13.877	−3.077	0.012*
CMCase × β–glucosidase ($X_2 \times X_3$)	35.627	7.899	0.000*

Source	DF	SS	MS	*F*–value	*p*–value
(B) ANOVA for quadratic model					
Regression	9	71064.2	7896.0	48.52	0.000
Linear	3	36103.4	7740.5	47.56	0.000
Square	3	36103.4	12034.5	73.95	0.000
Interaction	3	11739.3	3913.1	24.04	0.000
Residual (Error)	10	1627.5	162.7		
Lack of fit	5	273.1	54.6	0.20	0.948
Pure error	5	1354.3	270.9		
Total	19	72691.7			

DF – degrees of freedom; SS – sum of squares; MS – mean square.
* Significant *p*-value, $p \leqslant 0.05$; $R^2 = 0.9776$; predicted $R^2 = 0.9440$; adjusted $R^2 = 0.9575$.

$$[G_x^f] = \frac{[G_x]}{1 + \varepsilon(1 + \boldsymbol{\beta}[G_s])[\frac{1}{\delta} + \frac{1}{\delta}\frac{1}{\eta}][E^f]} \tag{8}$$

represents the number of cellulose sites covered by an adsorbed or complexed enzyme. Similarly, material balance of enzyme species yields following expression:

$$[E^f] = \frac{[E]}{(1 + \boldsymbol{\beta}[G_z]\left(1 + \left[\frac{1}{\delta} + \frac{1}{\delta}\frac{1}{\eta}\right][G_x^f]\right)} \tag{9}$$

Successive substitution and elimination $[EG_x]$ in the preceding equations gives the expression for reaction velocity as:

$$v = \frac{d[G_s]}{dt} = \frac{\boldsymbol{\kappa}[G_x][E]\left(\frac{1}{1+\beta[G_s]}\right)}{\boldsymbol{\alpha} + \boldsymbol{\phi}[G_x] + \varepsilon[E]} \tag{10}$$

where,

$$\boldsymbol{\kappa} = \frac{k}{\eta + 1} \text{ and } \boldsymbol{\alpha} = \frac{\eta\delta}{\eta + 1} \tag{11}$$

The factor $\boldsymbol{\phi}$ signifies extent of enzyme adsorption onto cellulose.

$$\boldsymbol{\phi} = \frac{[G_x^f]}{[G_x]} = \frac{\text{free cellulose sites}}{\text{total cellulose sites}} \tag{12}$$

$[G_x^f]$ can be obtained in terms of known quantities by substituting for $[E^f]$ (Eq. (9)) in equation for $[G_x^f]$ (Eq. (8)). This yields a quadratic in terms of $[G_x^f]$ as:

$$0 = -[G_x^f]^2 + ([G_x] - \boldsymbol{\alpha} - \varepsilon[E])[G_x^f] + \boldsymbol{\alpha}[G_x] \tag{13}$$

The positive root of above expression is:

$$\boldsymbol{\phi} = \frac{[G_x] - \boldsymbol{\alpha} - \varepsilon[E] + \sqrt{([G_x] - \boldsymbol{\alpha} - \varepsilon[E])^2 + 4\boldsymbol{\alpha}[G_x]}}{2[G_x]} \tag{14}$$

Alternatively, $\boldsymbol{\phi}$ can be directly evaluated by substituting for $[G_x^f]$ in equation for $\boldsymbol{\phi}$ as:

$$\boldsymbol{\phi} = \frac{\boldsymbol{\alpha}}{\boldsymbol{\alpha} + \varepsilon(1 + \boldsymbol{\beta}[G_s])\,[E^f]} \tag{15}$$

In order to make the calculations easier, Holtzapple et al. (1984) have used in the analysis concentrations for all quantities in g/L. The following values of different species were used for simulation of enzymatic hydrolysis using HCH-1 model: pretreated biomass (or cellulose) concentration = 38.8 g/L, cellulase concentration = 46.06 g/L (calculated on the basis of: specific activity = 1 U/mg, protein content estimated by Lowry's method (1951) = 1.7 g/L, and optimized concentration = 600 U/g pretreated biomass), β–glucosidase concentration = 7.76 g/L (calculated on the basis of: specific activity = 250 U/g and optimized concentration = 600 U/g pretreated biomass). HCH-1 model assumes that a single enzyme used in hydrolysis having both endoglucanase and cellobiase activity. In view of this, the enzyme concentration used during simulations is 24.91 g/L which is the average of cellulase and β–glucosidase concentration mentioned above. The expression for reaction velocity (Eq. (10)) contains 4 parameters, viz., $\boldsymbol{\alpha}$, $\boldsymbol{\beta}$, ε and $\boldsymbol{\kappa}$, which characterize kinetics and physiology of the enzymatic hydrolysis process. Comparison of the numerical solution of the ordinary differential equation (ODE) for reaction velocity with experimental profile of total reducing sugar (which represents the soluble product, G_s) gives physical insight into ultrasound-assisted enzymatic hydrolysis.

In order to match the experimental and simulated profile for the soluble product of hydrolysis, optimum values of the parameters in the ODE for hydrolysis velocity (Eq. (10)) need to be determined. This ODE was solved using Runge–Kutta 4th order method. The optimum values of the model parameters were determined by calculating root mean square (RMS) error between experimental values and model results using Genetic Algorithm (GA). The objective function for optimization was defined on the basis of squared error as:

$$obj = \min\left[\sum_{i=1}^{n} er_i\right] \tag{16}$$

where, n is the number of data points for reducing sugar concentration. The error term, er, is defined as:

$$er = \left(G_s^{\exp} - G_s^{\text{model}}\right)^2 \tag{17}$$

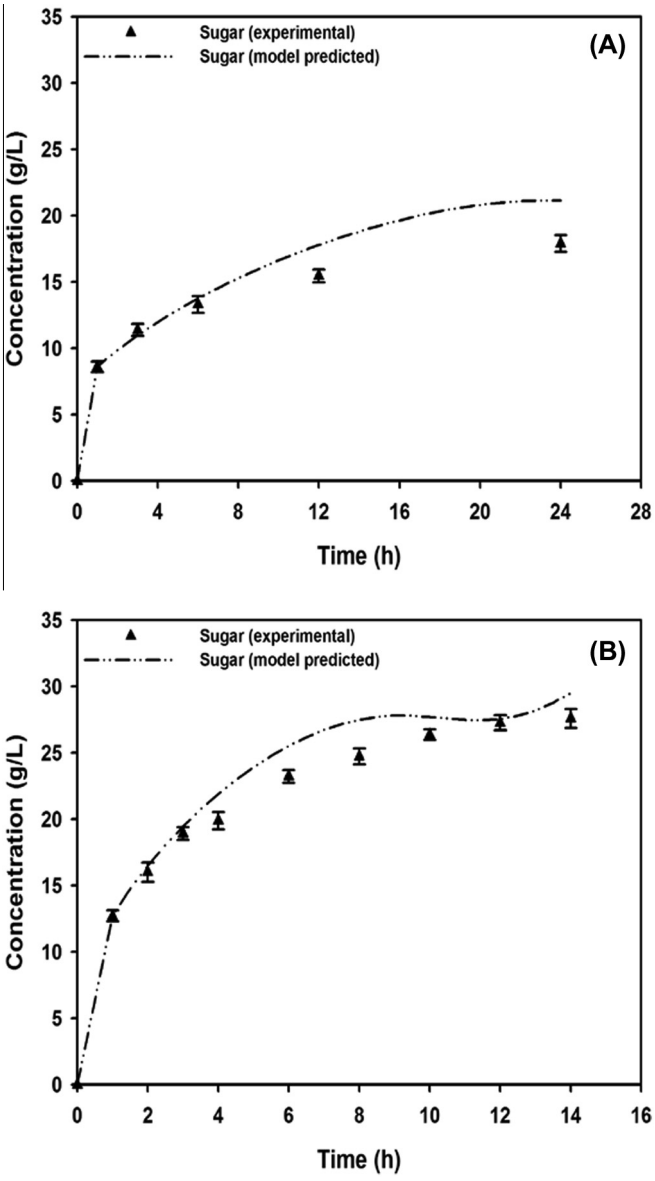

Fig. 2. Comparison of time profiles of total reducing sugar in enzymatic hydrolysis of pretreated *P. hysterophorus* biomass obtained experimentally (under optimum conditions obtained through CCD experimental design) and predicted by HCH-1 model. (A) Results for control experiment (with mechanical agitation). (B) Results for test experiment (with ultrasound irradiation).

The Genetic Algorithm minimizes the objective function and gives the optimized values of model parameters. A quantitative comparison of the model parameters for control and test experiments gives the mechanistic account of the influence of ultrasound on enzymatic hydrolysis of pretreated biomass.

4. Results and discussion

4.1. Optimization of enzymatic hydrolysis of P. hysterophorus biomass

4.1.1. Optimization by central composite experimental design

The full factorial CCD matrix of the optimization parameters is given in Table 1, which shows the response (i.e. reducing sugar yield) obtained in each experiment and the standard deviation. The second-order regression equation fitted to this data is as follows:

$$Y_{\text{sugar yield}} = 360.420 + 11.813X_1 + 19.144X_2 + 34.559X_3 - 46.625X_1^2 + 5.348X_2^2 + 11.328X_3^2 - 2.347X_1X_2 - 13.877X_1X_3 + 35.627X_2X_3 \quad (18)$$

Table 1 also shows values of the response variable (i.e. total reducing sugar yield) predicted by the second-order model in each experiment in the CCD design. It could be seen that the experimental and model-predicted values of the total reducing sugar yield match well indicating that the model fits well to the experimental data. The overall regression coefficient (R^2) of the model was 0.9776 with adjusted coefficient of 0.9575. The predicted R^2 of 0.9440 is also in reasonable agreement with adjusted regression coefficient. Table 2B represents the ANOVA (analysis of variance) of the fitted model. The insignificant p-value of 0.948 for lack of fit implied that the model is significant.

The p-value of zero for all linear, square and interaction coefficients in the quadratic model for response variable indicated their significance. The lowest F–values for interaction coefficients in Eq. (18) suggest that the influence of biomass, CMCase and β–glucosidase concentrations on total sugar yield are rather independent with no interaction among them. The quadratic model in Eq. (18) shows maxima for response variable of total reducing sugar yield for following values of optimization parameters: biomass concentration = 38.8 g/L, CMCase concentration = 600 U/g of biomass and β–glucosidase concentration = 50 U/g of biomass. The maximum response (reducing sugar yield) predicted by the model under optimized concentrations of these three components was 599.96 mg/g. The validation of this prediction was done by carrying out experiments in triplicate as follows: The experiments were performed with 38.8 g/L delignified biomass loading in sodium citrate buffer (0.05 M, pH 5.0) supplemented with CMCase (concentration 600 U/g delignified biomass) and β–glucosidase (concentration 50 U/g delignified biomass). The reactions were carried out in 150 mL Erlenmeyer flask with total reaction volume of 25 mL. The flasks were incubated at 30 °C and 150 rpm in an incubator shaker (Orbitek, Scigenics Biotech). The profile of total reducing sugar concentration and saccharification yield under optimized conditions has been shown in Fig. 2A. Although the total time of treatment was 96 h, Fig. 2A shows profile only up to 24 h, as the rate of hydrolysis was very low after 24 h. This is indicated by sugar yield of 461.4 mg/g in first 24 h of treatment, and mere increment of 132 mg/g in sugar yield in subsequent 72 h of treatment. The experimental value of maximum reducing sugar yield obtained under optimized values of parameters was 593.4 ± 16.3 mg/g in 96 h of treatment, which was in good agreement with the predicted yield of 599.96 mg/g. The contour plots (obtained using quadratic model) depicting trends in the response variable (total reducing sugar yield) with optimization variables are shown in Fig. 3. The non-linear nature of the contour plot curves indicates interaction between optimization variables (or experimental parameters) during their influence on the response variable, i.e. yield of total reducing sugar. Fig. 3A and B depict that for a given concentration of enzyme, the total reducing sugar yield shows a maximum for an optimum value of biomass concentration. On either side of this optimum value, the yield of total reducing sugar falls. On the other hand, Fig. 3C indicates that sugar yield shows a monotonous rise with concentrations of both enzymes. Reduction in the total sugar yield at high biomass concentration could be attributed to increase in mass transfer limitations (due to reduced convection) of the hydrolysis process that causes hindrance to enzyme action at high biomass concentration.

4.2. Intensification of enzymatic hydrolysis by ultrasound

4.2.1. Experimental results

The results of ultrasound-assisted enzymatic hydrolysis are given in Fig. 2B. The total reducing sugar yield in ultrasound assisted enzymatic hydrolysis was 711.3 ± 18.6 mg/g within 14 h of treatment. Comparison of these values with results of control experiments (sugar yield of 593.4 ± 16.3 mg/g in 96 h of treatment)

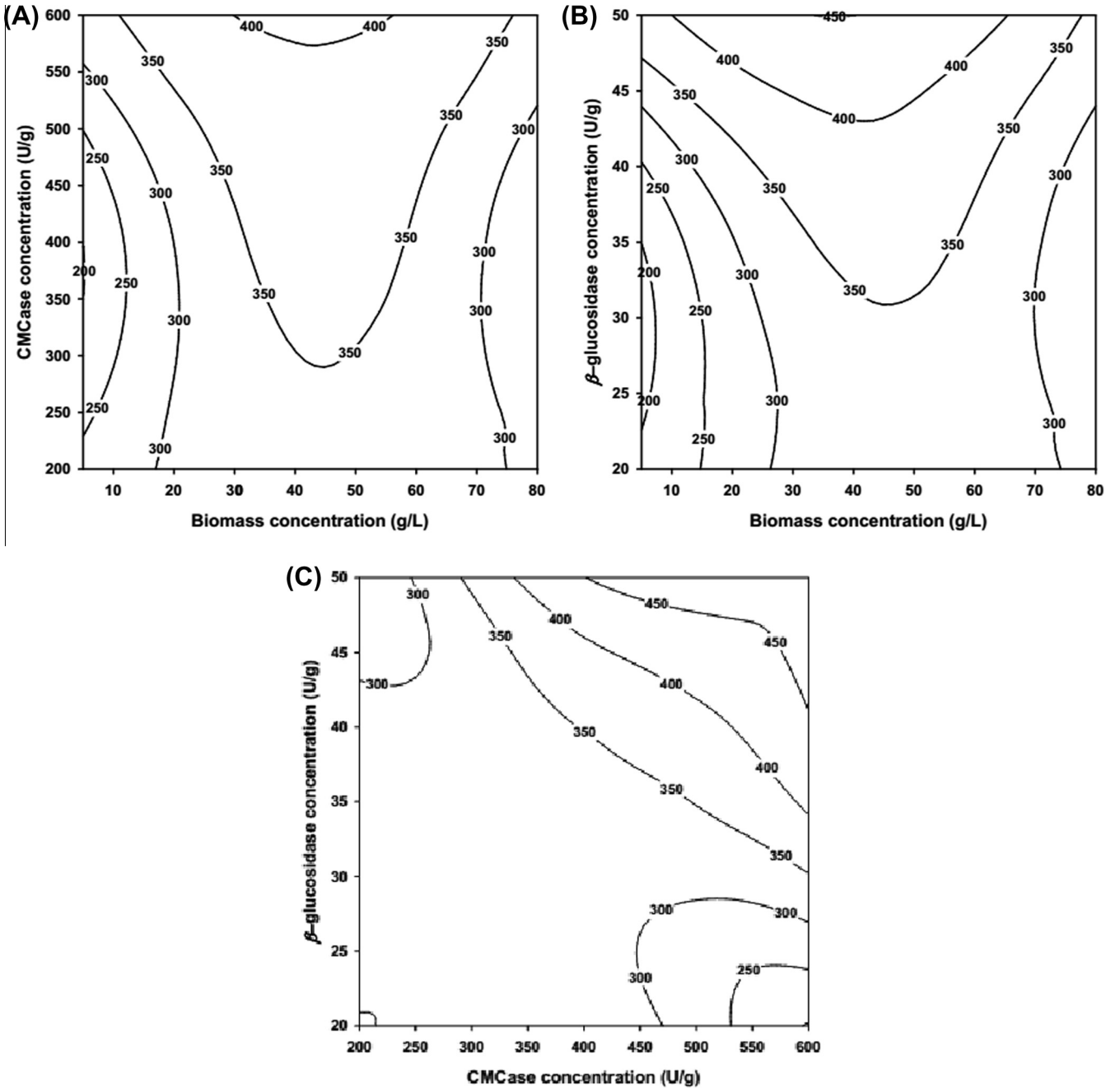

Fig. 3. Contour plots for reducing sugar yield showing the interactive effects of components of enzymatic hydrolysis: (A) concentrations of CMCase and Biomass, (B) concentrations of β–glucosidase and biomass, (C) concentrations of β–glucosidase and CMCase.

reveals that the kinetics of enzymatic hydrolysis was enhanced ~6×, while the total reducing sugar yield increased by ~20% with sonication. These enhancements are in concurrence with the findings of previous studies reported in literature. A comparative summary of the previous literature with the present study is given in Table 3. It could be observed that enhancement in the total reducing sugar yield with sonication in the present study is relatively less (~20%) as compared to literature. We attribute this discrepancy to relatively lower activity of the CMCase enzyme (obtained from natural isolate of *B. amyloliquefaciens* SS35) used in this study, as compared to commercial enzyme (with much higher activities) used in other studies.

4.3. Simulations and mechanistic analysis

The mechanistic analysis of ultrasound enhancement of enzymatic hydrolysis was done using two approaches, viz. Lineweaver–Burk analysis and fitting of experimental results to HCH-1 model using Genetic Algorithm. The results of Lineweaver–Burk analysis are given in Fig. 4 and the values of model parameters, viz. K_m and V_{max}, have been listed in Table 4A. Comparative evaluation of the values of K_m and V_{max} reveals that sonication not only increases the enzyme/substrate affinity (indicated by reduction in K_m), but also enhances conversion of enzyme/substrate complex into product, as indicated by increase in reaction velocity, V. Reduction in K_m (Michaelis constant or substrate concentration required to achieve half of maximum reaction velocity, V_{max}), is a consequence of faster transport and enhanced interaction of enzymes with substrate. This is attributed to the micro-turbulence and intense micro-mixing generated by ultrasound and cavitation in the reaction mixture. Enhancement in maximum reaction velocity, V_{max}, is also a consequence of the

Table 3
Comparative assessment of results obtained from ultrasound assisted enzymatic hydrolysis with published literature.

Enzyme	Sonication parameters	Observations and major results	Reference
Commercial cellulase	600 W, 20 kHz, Intensity 11.8 W/cm^2, 20% duty cycle	K_m decreased by 67.6%, V_{max} increased by 37%	Sulaiman et al. (2013)
Commercial cellulase	20 kHz, Intensity 17.33 W/cm^2, 30 min	Enzyme activity increased by 25%	Subhedar and Gogate (2014)
Commercial cellulase complex	132 W, 40 kHz, 240 min	Sugar yield increased to twofold	Lunelli et al. (2014)
Commercial cellulase	60 W, 70% duty cycle, 6.5 h	~2.4-fold enhancement in sugar yield	Subhedar et al. (2015)
Cellulase + β–glucosidase	35 W, 35 kHz, 10% duty cycle	K_m decreased by ~43%, V_{max} increased by ~21.7%, sugar yield increased by ~20%	This study

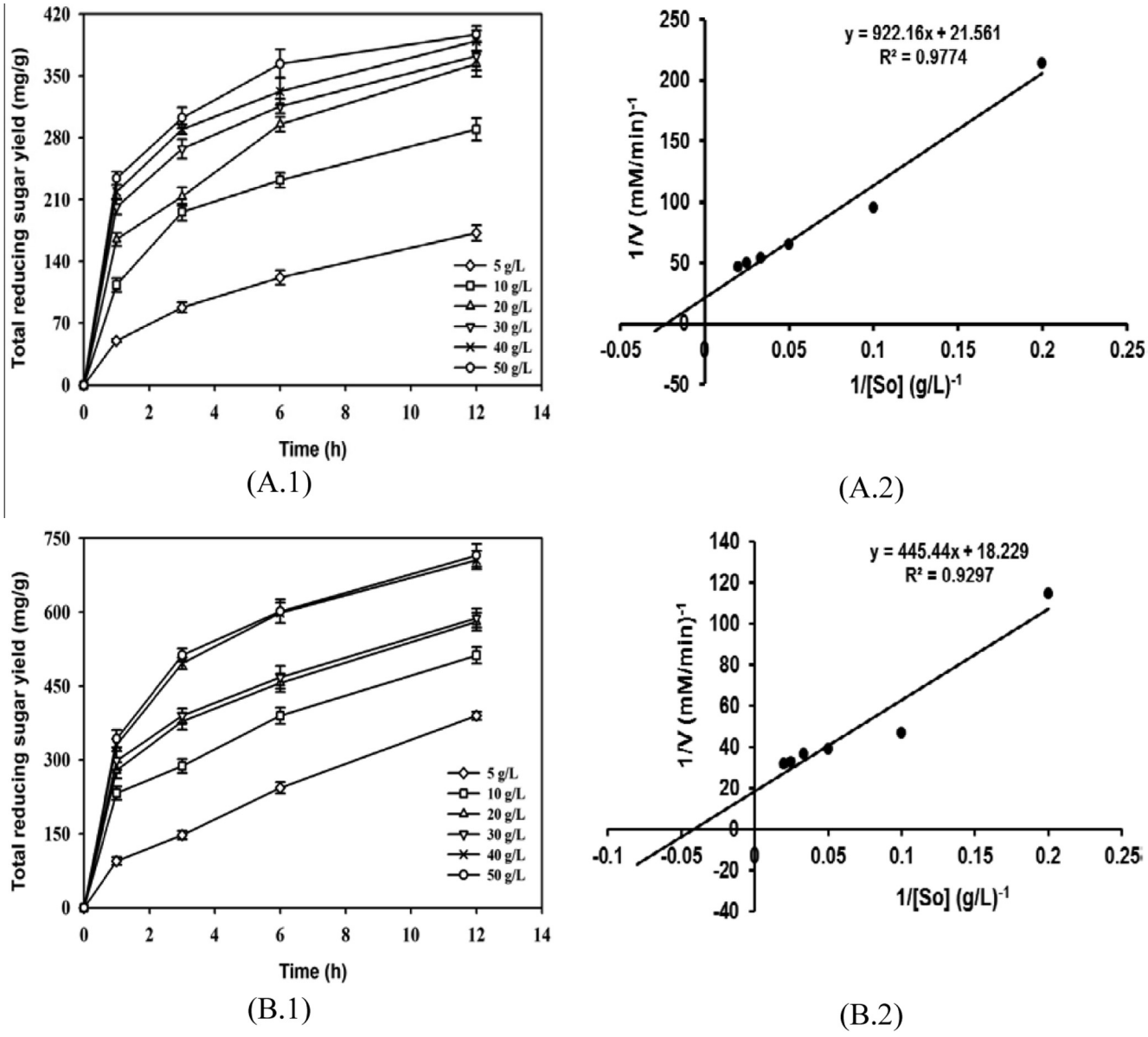

Fig. 4. Kinetic analysis of enzymatic hydrolysis using Lineweaver–Burk method. (A.1) Time profiles of reducing sugar yield at different biomass concentrations, (A.2) Lineweaver–Burk plot for control experiments (with mechanical agitation), and (B.1) time profiles of reducing sugar yield at different biomass concentrations, (B.2) Lineweaver–Burk plot for control experiments (with ultrasound).

physical effect of micro-convection, which helps faster splitting of the enzyme-substrate complex, and diffusion of the soluble product into the bulk.

The results of simulations of enzymatic hydrolysis under control (mechanical agitation) and test (ultrasound-assisted) conditions are depicted in Fig. 2, along with experimental profiles of

Table 4
Simulation results of enzymatic hydrolysis.

Experiment	K_m (g/L)	V_{max} (mM/min)
(A) Lineweaver–Burk analysis (enzyme kinetic parameters)		
Control (mechanical agitation)	42.77	0.046
Test (with ultrasound)	24.44	0.055
Parameter	Control experiment (mechanical agitation)	Test experiment (with ultrasound)
(B) Analysis with HCH-1 model with GA optimization		
Lumped kinetic constant of enzymatic hydrolysis, κ (h^{-1})	0.31	1.22
Lumped constant for enzyme/substrate complexation, α (g/L)	0.49	0.19
Product binding constant, β (L/g)	1.01	0.76
Number of cellulose sites covered by adsorbed or complexed enzyme, ϕ	0.17	0.19
Best fitness value for the model parameters	5.71	4.3

sugar yield. It could be seen that the experimental and simulated time profiles of total reducing sugar yield in hydrolysis under both control and test conditions match quite well. The values of the parameters of the HCH-1 model for the simulated profile obtained using GA optimization are listed in Table 4B. Comparative evaluation of the parameters of HCH-1 model under control and test conditions reveals following effects of sonication on hydrolysis:(1) Increase in lumped kinetic constant (κ) of hydrolysis(2) Reduction in lumped constant for enzyme/substrate complexation (α)(3) Reduction in the product binding constant β (indicative of extent of product inhibition)(4) Quite interestingly, the extent of adsorption of the enzyme on cellulose sites does not alter with sonication. Increase in κ and reduction in α can be explained along similar lines as the trends in K_m and V_{max} in Lineweaver–Burk analysis. Reduction in product binding constant is also attributed to strong micro-mixing induced by ultrasound and cavitation, due to which the product (glucose) is transported away from cellulose surface and diluted in the medium. This phenomenon reduces the probability of binding of product to the active site of the enzyme resulting in inhibition. Similar values of ϕ in both control and test experiments indicate that mass transfer is not limiting factor for enzyme adsorption on cellulose, which is in exact concurrence with the analysis and conclusion of Holtzapple et al. (1984). This result also points that increase in κ and reduction in α, are related to the action of β–glucosidase, which converts the dimers of cellobiose to monomeric sugar in bulk liquid medium. The net effect of the variations in κ, α and β is fourfold increase in kinetics of enzymatic hydrolysis with sonication. The total yield of reducing sugar shows only marginal improvement of ~20%. We attribute this result to the dependence of the hydrolysis process on the concentration of both the enzymes, i.e. process to be enzyme limiting. Although the enzyme concentrations were optimized prior to sonication, the optimum values of both concentrations obtained from CCD analysis were the maximum values used in the experimental design. A possible reason for marginal rise of ~20% in the reducing sugar yield could be ultrasound-induced enhancement in the activity of cellulase due to conformational changes in enzyme molecules (Subhedar and Gogate, 2014). This conformational change is also attributed to generation of intense micro-turbulence by ultrasound and cavitation in the liquid adjacent to the enzyme molecules (Subhedar and Gogate, 2014). This is, of course, a conjecture, which needs further detailed investigations and substantiation. Thus, the trends in kinetic and physiological parameters of HCH-1 model help in getting a mechanistic insight into the effect of ultrasound on enzymatic hydrolysis.

5. Conclusions

This study has given mechanistic insight into ultrasonic enhancement in enzymatic hydrolysis of pretreated and delignified biomass of *P. hysterophorus*. Analysis of hydrolysis using HCH-1 model reveals that intense micro-convection induced by ultrasound/cavitation enhances enzyme/substrate affinity and reaction velocity, in addition to reduction in product inhibition of enzymes. As a consequence, the kinetics of enzymatic hydrolysis shows 6× enhancement with sonication. However, hydrolysis process is revealed to be enzyme limited as per results of statistical experimental design. Marginal rise of ~20% in sugar yield with sonication is attributed to possible enhancement in enzyme activity by ultrasound.

Acknowledgements

Authors gratefully acknowledge valuable discussion with and suggestions from Prof. Mark T. Holtzapple (Department of Chemical Engineering, Texas A&M University, USA) regarding HCH-1 model analysis. Authors acknowledge the HPLC facility at Department of Chemical Engineering, I.I.T. Guwahati. Authors also thank anonymous referees of this paper for their meticulous evaluation and constructive criticism.

References

Beszédes, S., László, Z., Horváth, Z.H., Szabó, G., Hodúr, C., 2011. Comparison of the effects of microwave irradiation with different intensities on the biodegradability of sludge from the dairy- and meat-industry. Bioresour. Technol. 102, 814–821.

Bharadwaja, S.T.P., Singh, S., Moholkar, V.S., 2015. Design and optimization of a sono-hybrid process for bioethanol production from *Parthenium hysterophorus*. J. Taiwan Inst. Chem. Eng. http://dx.doi.org/10.1016/j.jtice.2015.01.022.

Chakma, S., Moholkar, V.S., 2011. Mechanistic features of ultrasonic desorption of aromatic pollutants. Chem. Eng. J. 175, 356–367.

Ghosh, S., Haldar, S., Ganguly, A., Chatterjee, P.K., 2013. Investigations on the kinetics and thermodynamics of dilute acid hydrolysis of *Parthenium hysterophorus* L. substrate. Chem. Eng. J. 229, 111–117.

Holtzapple, M.T., 1981. The pretreatment and enzymatic saccharification of Poplar wood (Ph.D. thesis). Department of Chemical Engineering, University of Pennsylvania, USA.

Holtzapple, M.T., Caram, H.S., Humphrey, A.E., 1984. The HCH–1 model of enzymatic cellulose hydrolysis. Biotechnol. Bioeng. 26, 775–780.

Khanna, S., Jaiswal, S., Goyal, A., Moholkar, V.S., 2012. Ultrasound enhanced bioconversion of glycerol by *Clostridium pasteurianum*: a mechanistic investigation. Chem. Eng. J. 200–202, 416–425.

Khanna, S., Jaiswal, S., Goyal, A., Moholkar, V.S., 2013. Mechanistic investigation of ultrasonic enhancement of glycerol bioconversion by immobilized *Clostridium pasteurianum* on silica support. Biotechnol. Bioeng. 110, 1637–1645.

Lowry, O.H., Rosebrough, N.J., Farr, A.L., Randall, R.J., 1951. Protein measurement with the Folin phenol reagent. J. Biol. Chem. 193, 265–275.

Lunelli, F.C., Sfalcin, P., Souza, M., Zimmermann, E., Pra, V.D., Foletto, E.L., Jahn, S.L., Kuhn, R.C., Mazutti, M.A., 2014. Ultrasound–assisted enzymatic hydrolysis of sugarcane bagasse for the production of fermentable sugars. Biosyst. Eng. 124, 24–28.

Malani, R.S., Khanna, S., Moholkar, V.S., 2013. Sonoenzymatic decolourization of an azo dye employing immobilized horse radish peroxidase (HRP): a mechanistic study. J. Hazard. Mat. 256–257, 90–97.

Moholkar, V.S., Sable, S.P., Pandit, A.B., 2000. Mapping the cavitation intensity in an ultrasonic bath using the acoustic emission. AIChE J. 46, 684–694.

Moholkar, V.S., Huitema, M., Rekveld, S., Warmoeskerken, M.M.C.G., 2002. Characterization of an ultrasonic system using wavelet transforms. Chem. Eng. Sci. 57, 617–629.
Nelson, N., 1944. A photometric adaptation of the Somogyi method for the determination of glucose. J. Biol. Chem. 153, 375–380.
Palacios-Bereche, R., Ensinas, A., Modesto, M., Nebra, S.A., 2014. New alternatives for the fermentation process in the ethanol production from sugarcane: extractive and low temperature fermentation. Energy 70, 595–604.
Pandiyan, K., Tiwari, R., Rana, S., Arora, A., Singh, S., Saxena, A.K., Nain, L., 2014. Comparative efficiency of different pretreatment methods on enzymatic digestibility of *Parthenium* sp. World J. Microbiol. Biotechnol. 30, 55–64.
Patel, S., 2011. Harmful and beneficial aspects of *Parthenium hysterophorus*: an update. 3 Biotech. 1, 1–9.
Patidar, R., Khanna, S., Moholkar, V.S., 2012. Physical features of ultrasound assisted enzymatic degradation of recalcitrant organic pollutants. Ultrason. Sonochem. 19, 104–118.
Rana, S., Tiwari, R., Arora, A., Singh, S., Kaushik, R., Saxena, A.K., Dutta, S.C., Nain, L., 2013. Prospecting *Parthenium* sp. pretreated with *Trametes hirsuta*, as a potential bioethanol feedstock. Biocatal. Agricu. Biotechnol. 2, 152–158.
Singh, S., Moholkar, V.S., Goyal, A., 2013. Isolation, identification and characterization of a cellulolytic *Bacillus amyloliquefaciens* strain SS35 from rhinoceros dung. ISRN Microbiol., Article ID 728134, 7p.
Singh, S., Bharadwaja, S.T.P., Yadav, P.K., Moholkar, V.S., Goyal, A., 2014a. Mechanistic investigation in ultrasound–assisted (alkaline) delignification of *Parthenium hysterophorus* biomass. Ind. Eng. Chem. Res. 53, 14241–14252.
Singh, S., Khanna, S., Moholkar, V.S., Goyal, A., 2014b. Comparative assessment of pretreatment strategies for enzymatic saccharification of *Parthenium hysterophorus*. Appl. Energy 129, 195–206.
Singh, S., Sarma, S., Agarwal, M., Goyal, A., Moholkar, V.S., 2015a. Ultrasound enhanced ethanol production from *Parthenium hysterophorus*: a mechanistic investigation. Bioresour. Technol. 188, 287–294.
Singh, S., Agarwal, M., Sarma, S., Goyal, A., Moholkar, V.S., 2015b. Mechanistic insight into ultrasound induced enhancement of simultaneous saccharification and fermentation of *Parthenium hysterophorus* for ethanol production. Ultrason. Sonochem. 26, 249–256.
Singh, S., Dikshit, P.K., Moholkar, V.S., Goyal, A., 2015c. Purification and characterization of acidic cellulase from *Bacillus amyloliquefaciens* SS35 for hydrolyzing *Parthenium hysterophorus* biomass. Environ. Progress Sustain. Energy 34, 810–818.
Sivasankar, T., Paunikar, A.W., Moholkar, V.S., 2007. Mechanistic approach to enhancement of the yield of a sonochemical reaction. AIChE J. 53, 1132–1143.
Somogyi, M., 1945. A new reagent for the determination of sugars. J. Biol. Chem. 160, 61–68.
Subhedar, P.B., Gogate, P.R., 2014. Enhancing the activity of cellulase enzyme using ultrasonic irradiations. J. Mol. Catal. B: Enzym. 101, 108–114.
Subhedar, P.B., Babu, N.R., Gogate, P.R., 2015. Intensification of enzymatic hydrolysis of waste newspaper using ultrasound for fermentable sugar production. Ultrason. Sonochem. 22, 326–332.
Sulaiman, A.Z., Ajit, A., Chisti, Y., 2013. Ultrasound mediated enzymatic hydrolysis of cellulose and carboxymethyl cellulose. Biotechnol. Prog. 29, 1448–1457.
Suresh, K., Ranjan, A., Singh, S., Moholkar, V.S., 2014. Mechanistic investigations in sono–hybrid techniques for rice straw pretreatment. Ultrason. Sonochem. 21, 200–207.
Suslick, K.S., 1990. Sonochemistry. Science 247, 1439–1445.
Timsina, B., Shrestha, B.B., Rokaya, M.B., Munzbergova, Z., 2011. Impact of *Parthenium hysterophorus* L. invasion on plant species composition and soil properties of grassland communities in Nepal. Flora Morphol. Distribution Funct. Ecol. Plants 206, 233–240.